Neuron, Vol. 43, 19–30, July 8, 2004, Copyright ©2004 by Cell Press

# Amyotrophic Lateral Sclerosis-Associated SOD1 Mutant Proteins Bind and Aggregate with Bcl-2 in Spinal Cord Mitochondria

**Piera Pasinelli,[1,2,*] Mary Elizabeth Belford,[1,2] Niall Lennon,[1,2] Brian J. Bacskai,[2] Bradley T. Hyman,[2] Davide Trotti,[1,2] and Robert H. Brown, Jr.[1,2,*]**

[1]Day Laboratory for Neuromuscular Research
[2]Department of Neurology
Harvard Medical School
Mass General Institute for Neurodegenerative Disease
Massachusetts General Hospital
Charlestown, Massachusetts 02129

## Summary

**Familial amyotrophic lateral sclerosis (ALS)-linked mutations in the copper-zinc superoxide dismutase (SOD1) gene cause motor neuron death in about 3% of ALS cases. While the wild-type (wt) protein is anti-apoptotic, mutant SOD1 promotes apoptosis. We now demonstrate that both wt and mutant SOD1 bind the anti-apoptotic protein Bcl-2, providing evidence of a direct link between SOD1 and an apoptotic pathway. This interaction is evident in vitro and in vivo in mouse and human spinal cord. We also demonstrate that in mice and humans, Bcl-2 binds to high molecular weight SDS-resistant mutant SOD1 containing aggregates that are present in mitochondria from spinal cord but not liver. These findings provide new insights into the anti-apoptotic function of SOD1 and suggest that entrapment of Bcl-2 by large SOD1 aggregates may deplete motor neurons of this anti-apoptotic protein.**

## Introduction

Amyotrophic lateral sclerosis is a fatal paralytic disorder characterized by selective death of motor neurons. About 3% of ALS cases are caused by mutations in the gene encoding copper-zinc superoxide dismutase (SOD1) (Rosen et al., 1993). More than 100 different mutations in SOD1 are known (Andersen et al., 2003). Mutant SOD1 (mutSOD1)-mediated toxicity results from a gain of one or more toxic properties that are not fully delineated (Cleveland and Rothstein, 2001).

While the wild-type (wt) SOD1 ($SOD1^{WT}$) is anti-apoptotic in neuronal cultures and a determinant of lifespan in *Drosophila* (Rothstein et al., 1994; Rabizadeh et al., 1995; Greenlund et al., 1995; Parkes et al., 1998), mutSOD1 proteins are pro-apoptotic both in vitro and in vivo (Durham et al., 1997; Rabizadeh et al., 1995; Ghadge et al., 1997; Pasinelli et al., 1998, 2000). Thus, increased expression of the pro-apoptotic proteins Bax and Bad and decreased expression of the anti-apoptotic Bcl-2 have been found in the spinal cord of transgenic mice expressing SOD1 with the G93A mutation (Vukosavic et al., 1999) and of human ALS patients without SOD1 mutations (Martin, 1999; Ekegren et al., 1999). In several different lines of ALS mice, several caspases are activated, including the upstream caspases 1 and 9 and the downstream executioner caspases 3 and 7 (Pasinelli et al., 1998, 2000; Vukosavic et al., 2000; Li et al., 2000; Guegan et al., 2001; Guegan and Przedborski, 2003). Release of cytochrome c from the mitochondria to the cytosol has been observed in spinal cords of $SOD1^{G93A}$ transgenic mice, linking mutSOD1-mediated toxicity to the mitochondrial apoptotic pathway (Guegan et al., 2001). In addition, survival of the $SOD1^{G93A}$ ALS mice is prolonged by overexpression of Bcl-2 (Kostic et al., 1997), by inhibition of caspase-1 (Friedlander et al., 1997), and by treatment with the pancaspase inhibitor ZVAD-fmk (Li et al., 2000). Biochemical changes associated with apoptosis have recently been reported in postmortem spinal cord tissues of ALS patients (Li et al., 2000; Ilzecka et al., 2001).

We have shown that an early event in mutSOD1-mediated apoptosis is activation of caspase-1 (Pasinelli et al., 2000). This is evident in the spinal cords of mice with three different SOD1 mutant transgenes. In one line of mice ($SOD1^{G85R}$), caspase-1 activation is the earliest molecular abnormality detected to date. These findings suggest that in mutSOD1-mediated cell death, apoptosis is a slowly evolving phenomenon that is directly triggered by the mutSOD1 protein. This observation, and the striking finding that $SOD1^{WT}$ protein is strongly anti-apoptotic, suggest that $SOD1^{WT}$ protects the cells against apoptosis either directly or indirectly by interacting with proteins that mediate programmed cell death, including members of the Bcl-2 family. The corollary prediction is that mutSOD1 protein may acquire a pro-apoptotic function by altering this interaction. An alternative model is that $SOD1^{WT}$ exerts its anti-apoptotic function by acting on the mitochondria and that mutSOD1 protein promotes cell death by an aberrant mitochondrial interaction.

Mitochondria are of particular interest in this context. First, mitochondrial degeneration, vacuolization, and swelling are characteristic pathological features in mutSOD1 mice and in familial ALS cases (Dal Canto and Gurney, 1995; Wong et al., 1995; Kong and Xu, 1998). Second, mitochondria tightly control apoptosis, and mutSOD1-mediated toxicity entails activation of the mitochondrial apoptotic pathway (Guegan et al., 2001). Third, although it has been considered a cytosolic protein, a fraction of SOD1 is localized in the mitochondria (Higgins et al., 2002; Okado-Matsumoto and Fridovich, 2002; Mattiazzi et al., 2002). Finally, mutSOD1 that is linked to mitochondria triggers apoptosis more strongly than the cytosolic mutant protein (Takeuchi et al., 2002).

To better characterize the mechanism by which SOD1 regulates apoptosis and to test the models described above, we have studied apoptotic proteins that interact with SOD1. We report here that the anti-apoptotic protein Bcl-2 interacts with both wt and mutSOD1. Moreover, we report binding of mutSOD1 to Bcl-2 in spinal cord mitochondria. Finally, we demonstrate that in mice

*Correspondence: ppasinelli@partners.org (P.P.), rhbrown@partners.org (R.H.B.)

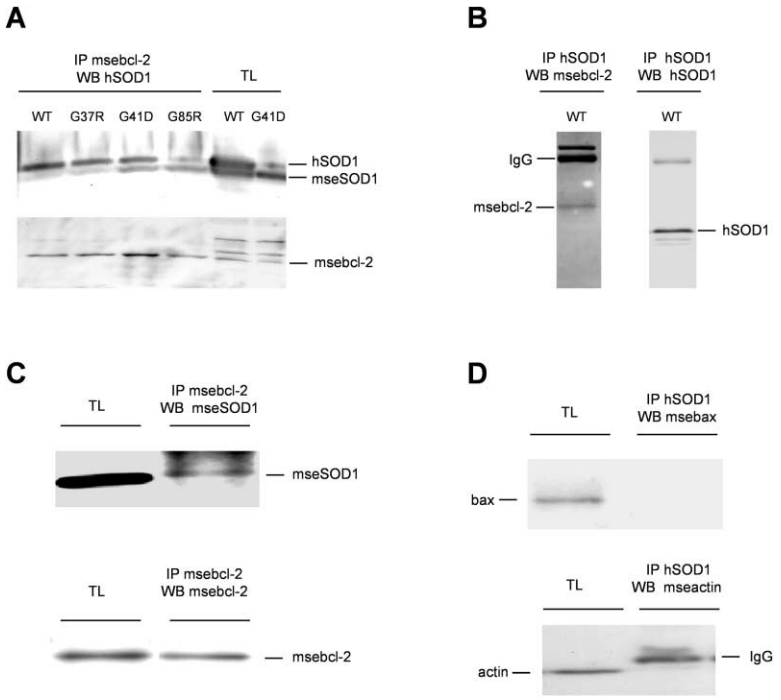


Figure 1. Wild-Type and mutSOD1 Coprecipitate with Bcl-2

(A) Co-immunoprecipitation was carried out with the anti-mouse Bcl-2 antibody. Western blot analysis of the immunoprecipitates using the anti-human SOD1 antibody indicates that Bcl-2 coprecipitates wt and mutSOD1s (G37R, G41D, and G85R) (top). Bcl-2 immunoprecipitation was confirmed by reprobing the membrane with the anti-mouse Bcl-2 antibody (bottom).

(B) The reverse immunoprecipitation was carried out with the anti-human SOD1 antibody. Western blot analysis with the anti-mouse Bcl-2 antibody (left) confirms the interaction between SOD1 and Bcl-2. The immunoblot was stripped and reprobed for the precipitating SOD1 (right).

(C) The anti-mouse Bcl-2 antibody coprecipitates the endogenous mouse SOD1 (top). The immunoblot was stripped and reprobed for the precipitating Bcl-2 (bottom).

(D) The anti-SOD1 antibody does not coprecipitate the anti-apoptotic protein Bax (top) or Actin (bottom). Abbreviations: TL, total lysates; hSOD1, human SOD1; msebcl-2, mouse Bcl-2.

and human spinal cords, Bcl-2 binds to high molecular weight SDS-resistant mutSOD1-containing aggregates that are present in spinal cord but not liver mitochondria. These observations suggest the hypothesis that mutant protein captures Bcl-2 within unstable aggregates, depleting the motor neurons of this anti-apoptotic protein.

## Results

### Wild-Type and Mutant SOD1 Associate with Bcl-2

Postnuclear homogenates from N2A cells transfected with either the wt human SOD1 or three different mutants (G37R, G41D, and G85R) were subjected to immunoprecipitation using an anti-mouse Bcl-2 antibody. Western blot analysis of immunoprecipitated proteins revealed that both wt and mutSOD1s were coprecipitated by the anti-mouse Bcl-2 antibody (Figure 1A, top), indicating a physical interaction between SOD1 and Bcl-2. The N2A cells also express the endogenous mouse SOD1. Because human SOD1 has a slower electrophoretic mobility than mouse SOD1, the two proteins are easily distinguishable on Western blots. As shown in Figure 1A (top), the anti-Bcl-2 antibody coprecipitates both the human SOD1 and the endogenous mouse protein. When the same blot was immunostained with an anti-Bcl-2 antibody, a single band of about 26 kDa corresponding to the endogenous mouse Bcl-2 was detected, indicating that Bcl-2 was successfully immunoprecipitated (Figure 1A, bottom). To confirm the binding between SOD1 and Bcl-2, we performed the reverse experiment in $hSOD1^{WT}$-expressing cells. The presence of Bcl-2 in the SOD1 immunoprecipitate was shown by Western blot analysis (Figure 1B, left), and SOD1 immunoprecipitation was confirmed on the same blot restained with the anti-human SOD1 antibody (Figure 1B, right).

To verify that endogenous Bcl-2 can associate with endogenous SOD1 and that the interaction is not an artifact of overexpression of the human SOD1 protein, we incubated lysates from naive, nontransfected N2A cells with the anti-mouse Bcl-2 antibody. The immunoprecipitate was analyzed by Western blot for the presence of the endogenous mouse SOD1. Figure 1C (top) shows that the anti-Bcl-2 antibody coprecipitated endogenous mouse SOD1. Bcl-2 immunoprecipitation was confirmed by restaining the same blot with anti-mouse Bcl-2 antibody (Figure 1C, bottom). This result confirms the positive immunostaining for both human and mouse SOD1 that we have observed in the immunoprecipitates shown in Figure 1A and clearly shows that endogenous SOD1 associates with endogenous Bcl-2.

To demonstrate the specificity of the interaction between SOD1 and Bcl-2, we performed co-immunoprecipitation experiments with the anti-human SOD1 antibody and analyzed the resulting immunoprecipitates by Western blot with an anti-Bax and an anti-Actin antibody as negative controls. Lysates from wt human SOD1-expressing N2A cells were immunoprecipitated for SOD1. Bax and Actin were not immunodetected in the immunoprecipitates but were present in the straight lysates (Figure 1D). Similarly, the anti-mouse Bcl-2 antibody was unable to precipitate Actin (data not shown).

### SOD1 and Bcl-2 Interact In Vivo in Spinal Cord of Transgenic SOD1 Mice and in Human Spinal Cords

We confirmed the physical interaction between SOD1 and Bcl-2 in spinal cord homogenates of transgenic SOD1 mice overexpressing either wt human SOD1 or G93A mutant SOD1 and in human spinal cord homogenates. Spinal cord homogenates from presymptomatic G93A ALS mice and age-matched transgenic mice overexpressing human $SOD1^{WT}$ were subjected to immu-

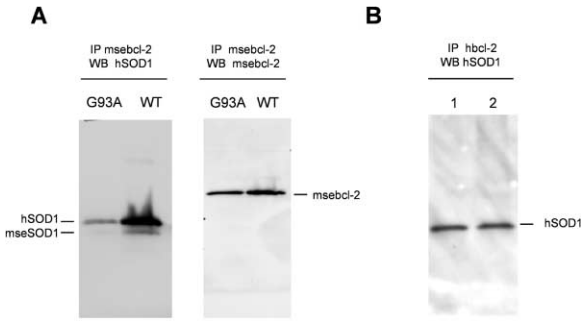


Figure 2. SOD1 and Bcl-2 Interact In Vivo in Mouse and Human Spinal Cords

(A) Spinal cord homogenates from presymptomatic (45 days old) $SOD1^{G93A}$ mice and age-matched $hSOD1^{WT}$ overexpressing mice were subjected to immunoprecipitation using the anti-mouse Bcl-2 antibody. Blots were probed with the anti-human SOD1 antibody (left) and subsequently the anti-mouse Bcl-2 antibody (right).

(B) Coprecipitation experiments were performed in human spinal cord homogenates with the anti-human Bcl-2 antibody. Bcl-2 precipitates stained positive for SOD1. Abbreviations: hSOD1, human SOD1; msebcl-2, mouse Bcl-2.

noprecipitation using the anti-mouse Bcl-2 antibody. Western blot analysis confirmed the presence of both human and mouse SOD1 in the precipitates (Figure 2A, left) and confirmed that Bcl-2 was successfully precipitated (Figure 2A, right). We then carried out a co-immunoprecipitation experiment in human spinal cords. Spinal cord homogenates from human samples were immunoprecipitated with an anti-human Bcl-2 antibody. Western blot analysis confirmed the presence of a positive SOD1 immunoreactive band in the precipitates (Figure 2B).

### Crosslinking Studies Show Formation of High Molecular Mass Complexes Containing SOD1 and Bcl-2

To validate our findings, we performed crosslinking experiments followed by off-diagonal two-dimensional (2D) electrophoresis. Lysates from human $SOD1^{WT}$-expressing N2A cells were incubated with the hydrophobic crosslinker DSP that allows analysis of intra- and intermembrane interactions. DSP is a thiol-cleavable, 12 Å crosslinker routinely used in 2D nonreducing/reducing diagonal gels. In this system, DSP-linked stabilized membrane complexes are first separated according to their electrophoretic mobility under nonreducing conditions. The first dimension lanes are then cut from the gel, reduced to cleave the crosslinked covalent bonds, and overlaid on top of the second dimension slab gel. Previously crosslinked complexes are identified as single dots that run off the diagonal. In the first dimension, increasing concentrations of crosslinker enhanced the appearance of high molecular mass complexes that stained positive on Western immunoblots for both Bcl-2 (Figure 3A, left) and SOD1 (Figure 3A, right). Silver staining of the second dimension run under reducing conditions showed two dots coming off the diagonal and migrating on the same vertical line. One dot migrated at about 26 kDa and the other migrated at about 17–20 kDa, corresponding to the molecular weights of Bcl-2 and SOD1, respectively (Figure 3B, bottom). Western blot replicas of the second dimension showed that the 26 and the 17–20 kDa positively immunostained with the anti-mouse Bcl-2 and with the anti-SOD1 antibody, respectively (Figure 3B, top), confirming the results obtained by silver staining. Similar results were obtained from crosslinking of lysates of cells expressing two different SOD1 mutants (G37R and G41D) (data not shown). We cannot exclude the formal possibility that crosslinking in these experiments is between Bcl-2 or SOD1 itself; indeed, it is well established that SOD1 homodimerizes. However, these crosslinking experiments are fully consistent with complex formation between Bcl-2 and SOD1 as suggested by the co-immunoprecipitation experiments above. Our next experiments provide additional support for this direct interaction.

### Fluorescence Lifetime Imaging Microscopy Analysis Confirms that SOD1 and Bcl-2 Interact in the N2A Cells

In these experiments, fluorescence lifetime imaging microscopy (FLIM) was used to monitor fluorescence resonance energy transfer (FRET) between fluorescein-labeled Bcl-2 (donor) and Cy3-labeled SOD1 (acceptor) in human $SOD1^{WT}$-expressing N2A cells. In cells, if protein-linked donor and acceptor fluorophores are in close proximity, FRET causes a reduction in the lifetime ($\tau$) of the fluorescence of the donor. FLIM allows detection of protein-protein interaction on a spatial scale (less than 10 nm) (Bacskai et al., 2003). The lifetime of fluorescein-conjugated secondary antibody to bind the primary anti-Bcl-2 antibody was calculated to be $2.1 \pm 0.18$ ns (Figure 3C). This was shortened to $1.09 \pm 0.3$ ns by the presence of the Cy3-conjugated secondary antibody bound to the anti-SOD1 primary antibody (Figure 3C), indicating that there is significant energy transfer (FRET) between the donor and the acceptor fluorophore because of the very close spatial interaction between SOD1 and Bcl-2. By contrast, when the Cy-3 antibody was bound to the anti-COX4 antibody to stain the mitochondria, there was no FLIM-detectable association between Bcl-2 and COX4 (Figure 3C). In vivo, double immunofluorescence experiments revealed that SOD1 and Bcl-2 colocalize extensively in the anterior horn motor neurons of presymptomatic $SOD1^{G93A}$ mice (not shown).

### SOD1 Directly Interacts with Bcl-2

To determine whether SOD1 directly binds to Bcl-2, we performed coprecipitation experiments using in vitro translated proteins. Bcl-2 cDNA as well as SOD1 cDNAs (wt and G93A) were translated in vitro as described. Figure 4 shows in vitro translated products of Bcl-2 (lane 1, left) and $SOD1^{WT}$ (lane 1, middle). As shown, [$^{35}$S]methionine radiolabeled Bcl-2 was first visualized by autoradiography. Because it lacks methionines, SOD1 cannot be detected by autoradiography. We therefore analyzed translation of the SOD1 protein by Western immunoblotting. Portions of the translated proteins were immunoprecipitated with the indicated antibodies. In the absence of SOD1 protein, the anti-human SOD1 antibody was not able to immunoprecipitate in vitro translated Bcl-2 (Figure 4, left, lane 2), indicating that the SOD1-specific antibody does not directly bind to

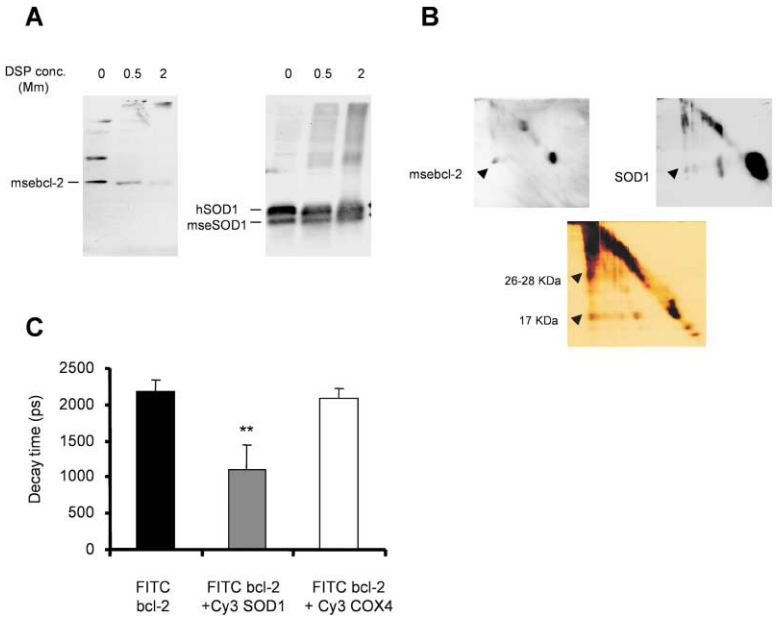


Figure 3. Crosslinking Analysis and Off Diagonal 2D Electrophoresis

(A and B) Crosslinking reaction was performed on N2A cell lysates, and samples were resolved on SDS-PAGE under (A) nonreducing (first dimension) and (B) reducing (second dimension) conditions. For the first dimension, the appearance of high molecular mass complexes was detected with both the anti-mouse Bcl-2 antibody (A, left) and anti-human SOD1 antibody (A, right). Western blot (B, top) and silver stain (B, bottom) analysis of the second dimension.

(C) FLIM was undertaken to determine the amount of FRET between FITC-labeled Bcl-2 (donor) and Cy3-labeled SOD1 or Cy3-labeled COX4 (acceptor). Data are mean ± SD of three independent observations. **$p < 0.001$.

Bcl-2 and therefore does not nonspecifically precipitate Bcl-2. Similarly, in the absence of Bcl-2, the anti-human Bcl-2 antibody was not able to immunoprecipitate SOD1 (Figure 4, middle, lane 2), while it successfully precipitated Bcl-2 (Figure 4, left, lane 3). This confirms the specificity of our previous coprecipitation experiments. When the anti-human SOD1 antibody was used to precipitate mixed portions of the two in vitro translated proteins, Bcl-2 was detected, confirming that SOD1 directly interacts with Bcl-2 (Figure 4, left, lane 4). Similarly, when mixed portions of translated human Bcl-2 and G93A mutant were precipitated with the anti-human Bcl-2 antibody, the mutSOD1 was detected with the anti-human SOD1 antibody (Figure 4, right). We confirmed the specificity of these immunoprecipitations by co-expressing FLAG-tagged human Bcl-2 and untagged human SOD1 in *Xenopus laevis* oocytes. The anti-FLAG antibody successfully pulled down human SOD1 (not shown).

## Wild-Type SOD1 Binds the N-Terminal Domain of Bcl-2, and Mutations in SOD1 Alter This Binding

To determine the regions of Bcl-2 that are required for specific binding to SOD1, we used a panel of human Bcl-2 mutants (generous gift from Dr. Stanley Korsmeyer). These include four deletion mutants (ΔBH4, Δloop, ΔTM, and ΔBH4/Δloop, lacking the BH4, loop, transmembrane, and BH4+loop domain, respectively) (Figure 5A). Using these mutants, we examined the regions of human Bcl-2 important for binding to SOD1 by co-immunoprecipitation of in vitro translated proteins. We mixed in vitro translated Bcl-2 mutants with either in vitro translated wt or $SOD1^{G93A}$ mutant and performed co-immunoprecipitation experiments with anti-human Bcl-2 antibody. Immunoprecipitates were analyzed by Western blot using the anti-human SOD1 antibody. $SOD1^{WT}$ coprecipitates with Δloop, ΔBH4, ΔTM, and wt Bcl-2 to the same extent. In contrast, the ΔBH4/Δloop

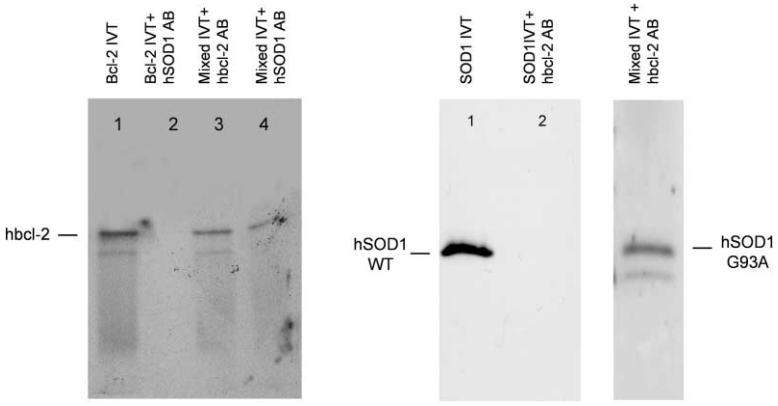


Figure 4. SOD1 and Bcl-2 Directly Interact In Vitro

Bcl-2 cDNA and SOD1 cDNAs (wt and G93A) were in vitro translated as described and proteins were analyzed either by autoradiography (Bcl-2, left) or by Western blot analysis (SOD1, middle and right). In vitro translated products of wt Bcl-2 (lane 1, left) and $SOD1^{WT}$ (lane 1, middle) are shown. To determine the specificity of either the anti-human Bcl-2 or the anti-human SOD1 antibody in immunoprecipitation, portions of the translated proteins (wt Bcl-2 and SOD1) were immunoprecipitated with anti-human SOD1 antibody or anti-human Bcl-2 antibody. The anti-SOD1 antibody did not precipitate human Bcl-2 (lane 2, left), and the anti-human Bcl-2 antibody failed to precipitate SOD1 (lane 2, middle). Mixed portions of the two in vitro translated proteins were positively immunoprecipitated by the anti-SOD1 antibody (lane 4, left) or the anti-Bcl-2 antibody (right). Abbreviation: IVT, in vitro translation.

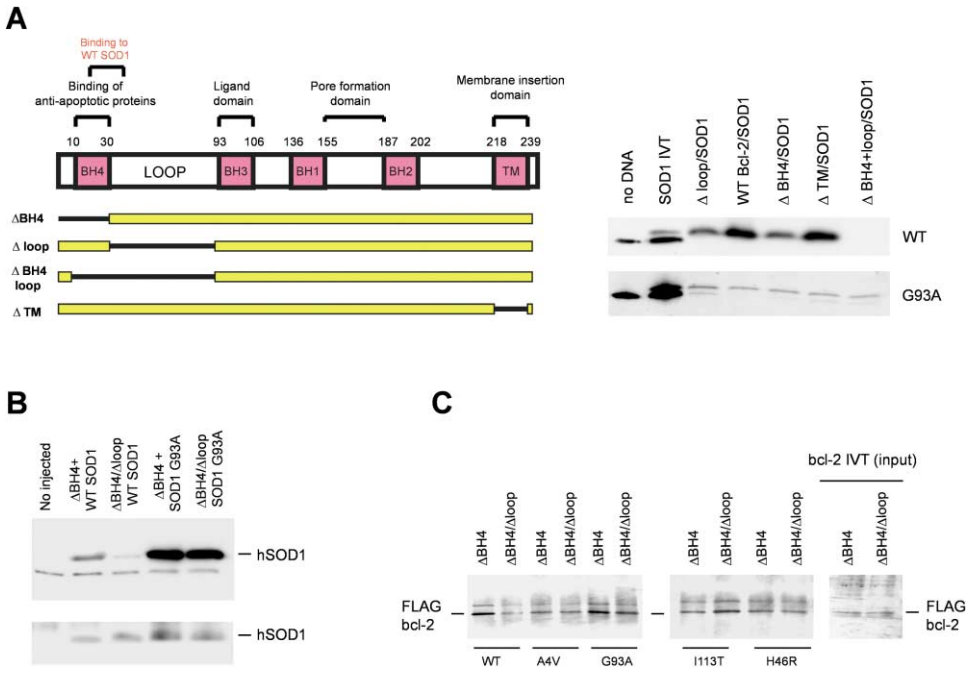


Figure 5. Wild-Type SOD1 Binds the N-Terminal Domain of Bcl-2

(A) A diagram of the Bcl-2 deletion mutants used is represented in the left panel. Right: In vitro translated wt or Bcl-2 mutants and wt or SOD1$^{G93A}$ mutant were mixed and immunoprecipitated with the anti-Bcl-2 antibody. Immunoprecipitates were analyzed by Western blot with the anti-SOD1 antibody.

(B) FLAG-tagged Bcl-2 and untagged SOD1 were co-expressed in *Xenopus* oocytes. The upper gel shows Western blot analysis of hSOD1 after immunoprecipitation with the anti-FLAG antibody. The lower picture shows Western blot analysis of hSOD1 in the total lysates to verify that SOD1 is expressed in oocytes.

(C) Bcl-2 deletion mutants and mutSOD1 cDNAs were in vitro translated. Mixed portions of translated proteins were immunoprecipitated with the anti-hSOD1 antibody. Western blot was analyzed with the anti-FLAG antibody.

double deletion abolishes the interaction (Figure 5A, right), indicating that the region between the BH4 and the loop domain of Bcl-2 is essential for the binding with SOD1$^{WT}$. However, the ΔBH4/Δloop double deletion does not abolish the binding with SOD1$^{G93A}$ mutant. In fact, SOD1$^{G93A}$ coprecipitates with all four Bcl-2 deletion mutants and wt Bcl-2 to a similar extent (Figure 5A, right). We also used two different mutants with single point mutations in the BH1 and BH2 domains. These point mutations abolish binding of Bcl-2 with other proteins (Yin et al., 1994; Sedlak et al., 1995). None of these Bcl-2 point mutations abolished the binding with either wt or SOD1$^{G93A}$ mutant (not shown). These data indicate that the region between the BH4 and the loop domain in Bcl-2 is required for the binding with SOD1 and that mutations in SOD1 alter this binding.

To confirm that the different binding to Bcl-2 observed between wt and mutSOD1 also occurs in a cellular system in which proteins are properly folded and targeted to the correct intracellular compartment, we used the *Xenopus laevis* oocytes expression system. Two FLAG-tagged Bcl-2 mutants (ΔBH4 and ΔBH4/Δloop double deletion) were co-expressed in oocytes with human SOD1 (wt and G93A). When the ΔBH4 deletion mutant was co-expressed with SOD1$^{WT}$, the anti-FLAG antibody was able to coprecipitate SOD1, while the ΔBH4/Δloop double deletion mutant abolished or greatly reduced the interaction with SOD1 (Figure 5B, left). On the contrary, when co-expressed with SOD1$^{G93A}$, both Bcl-2 mutants retained their binding ability (Figure 5B, left), confirming the in vitro experiments described above.

We further confirmed the generality of these findings using three other mutSOD1s (A4V, I113T, and H46R). In the first set of experiments, we mixed the in vitro translated FLAG-tagged ΔBH4 and ΔBH4/Δloop Bcl-2 mutants with in vitro translated SOD1s (wt, A4V, I113T, G93A, and H46R) and performed co-immunoprecipitation experiments using the anti-human SOD1 antibody. Analysis of the resulting immunoprecipitates with the anti-FLAG antibody confirmed our previous findings; all mutSOD1s equally coprecipitated with ΔBH4 and ΔBH4/Δloop Bcl-2, while this double Bcl-2 deletion greatly reduced the binding with SOD1$^{WT}$ (Figure 5C).

## Mutant SOD1 Forms SDS-Resistant High Molecular Weight Aggregates that Preferentially Bind to Spinal Cord Mitochondria and Coprecipitate with Bcl-2

We next analyzed whether mutations in SOD1 affect the interaction with Bcl-2 in vivo during disease progression in the SOD1$^{G93A}$ mice and in human ALS. Spinal cord homogenates from either ALS mice or mice overexpressing SOD1$^{WT}$ were subjected to immunoprecipitation using the anti-mouse Bcl-2 antibody. Immunoprecipitates were analyzed by Western blot using the anti-human SOD1 antibody. As the disease progressed in the SOD1$^{G93A}$ mice, there was a gradual increase in the amount of SOD1 coimmunoprecipitated by the anti-Bcl-2 antibody. When

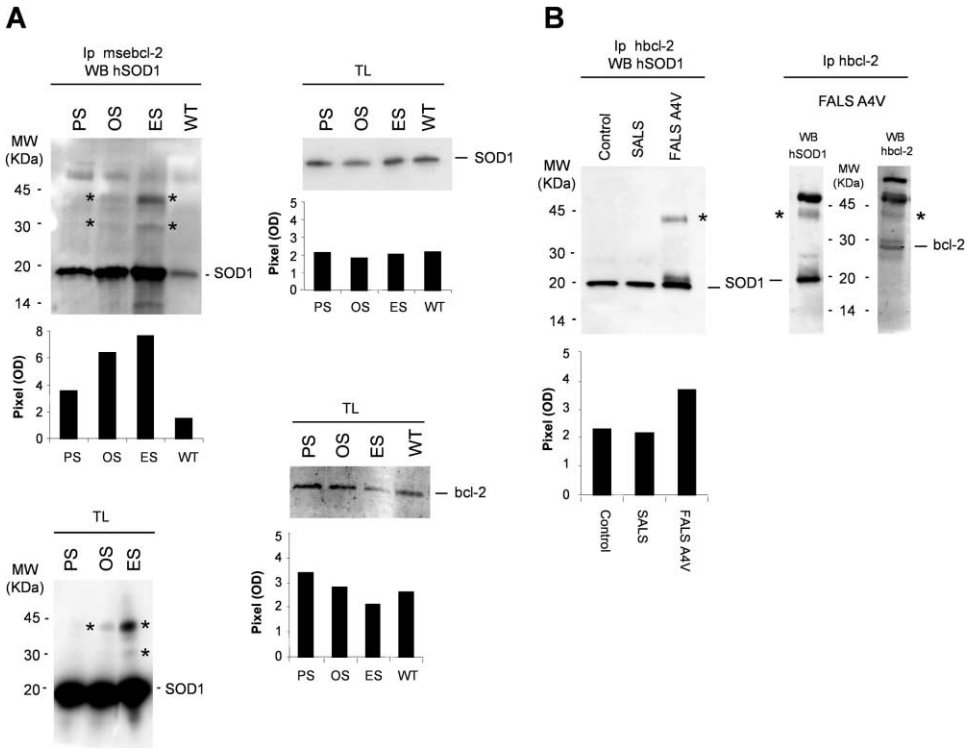


Figure 6. Bcl-2 Binds SDS-Resistant High Molecular Weight SOD1 Aggregates

(A) Spinal cord homogenates from SOD1$^{G93A}$ and hSOD1$^{WT}$ overexpressing mice were subjected to immunoprecipitation using the anti-Bcl-2 antibody, and precipitated samples were analyzed by Western blot using the anti-human SOD1 antibody. Left upper panel shows samples from presymptomatic (PS), early onset (OS), or end stage (ES) ALS mice and 140-day-old hSOD1$^{WT}$ overexpressing mice (age-matched with the end stage ALS mice). Left lower panel shows Western blot analysis of total lysates derived from the same mice stained with the anti-human SOD1 antibody and overexposed to detect the appearance of SDS-resistant high molecular weight aggregates (asterisks). Right panel shows Western blot analysis of total lysates derived from the same mice to confirm equal expression of SOD1 and Bcl-2 over time. Densitometric analysis was performed for each blot and is summarized in the histogram below each blot.

(B) Human spinal cord homogenates were subjected to immunoprecipitation using an anti-human Bcl-2 antibody and samples analyzed by Western blot with the anti-human SOD1 antibody. Compared to non-ALS and sporadic controls, the SOD1-A4V ALS sample showed a stronger binding between SOD1 and Bcl-2 (see densitometric analysis below), and the Bcl-2 antibody coprecipitated high molecular weight SDS-resistant A4V containing aggregates (asterisks).

compared to that of presymptomatic mice, the amount of SOD1 precipitated by the anti-Bcl-2 antibody is 1.8- and 2.1-fold higher at the time of onset and end stage, respectively (Figure 6A, histogram). This is not due to an increase in overall SOD1 expression, since equal SOD1 expression is detected among the different animals (Figure 6A, upper right). This is also not due to an increase over time in Bcl-2 expression, because in fact this decreases as disease progresses (Figure 6A, lower right; Vukosavic et al., 1999). At the time of onset, and more at end stage, Bcl-2 binds high molecular weight SDS-resistant SOD1 aggregates (Figure 6A, left, asterisks). The time course of appearance of these precipitated aggregates and their levels of expression correlate with that of high molecular weight complexes that are present in the total lysates of these mice after a prolonged exposure of the blot (Figure 6A, lower left). As shown, the high molecular weight aggregates are hardly detectable in total lysates at the time of onset. However, the fact that they are precipitated with the Bcl-2 antibody strongly indicates that they tightly bind to Bcl-2.

Bcl-2 binding to large mutSOD1-containing aggregates is also observed in spinal cord homogenate of an ALS patient carrying the A4V mutation. The amount of SOD1 coprecipitated by the Bcl-2 antibody is about 1.5-fold higher in the SOD1-ALS patient than in a sporadic patient and non-ALS control (Figure 6B, left). Moreover, the anti-human Bcl-2 antibody is able to coprecipitate high molecular weight A4V-containing aggregates as observed in the mice. Bcl-2 is entrapped in these high molecular weight aggregates that stain positive for the anti-Bcl-2 antibody (Figure 6B, right).

We next determined whether the SOD1/Bcl-2-containing aggregates are present in the mitochondria. Bcl-2 is a membrane protein found in mitochondria, ER, and nuclei. A single transmembrane domain at the carboxyl terminus anchors Bcl-2 to the mitochondrial membrane while the majority of the protein faces the cytosol (Schimmer et al., 2001). Based on our in vitro experiments with Bcl-2 deletion mutants, we predicted that while SOD1$^{WT}$ binds the cytosolic portion of Bcl-2, mutSOD1 binds at or near the mitochondrial membrane. A corollary prediction is that the mutSOD1 protein is associated with the mitochondrion more tightly than SOD1$^{WT}$ during mitochondrial purification. Accordingly, when we isolated mitochondria from mouse and human

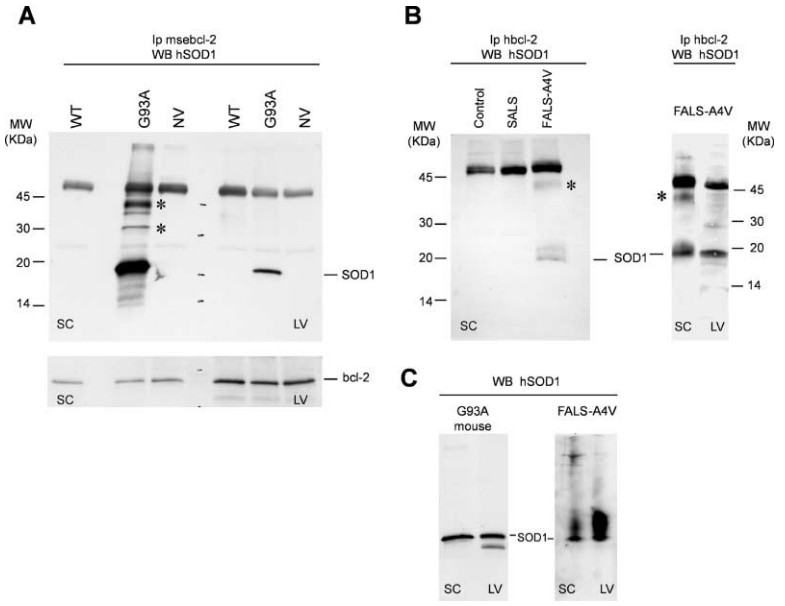


Figure 7. Mutant SOD1 Specifically Binds Bcl-2 in the Mitochondria

(A) Mitochondria purified from spinal cord and liver of 133-day-old naive (NV), hSOD1$^{WT}$ (wt), and SOD1$^{G93A}$ transgenic mice were incubated with the anti-mouse Bcl-2 antibody, and samples were analyzed by Western blot with the anti-human SOD1 antibody. The precipitating Bcl-2 was analyzed by Western blot using an anti-mouse Bcl-2 antibody (bottom).

(B) Immunoprecipitation with the anti-human Bcl-2 antibody was performed using human purified mitochondria. Immunoprecipitates were analyzed by Western blot. The left panel shows a representative Western blot of Bcl-2 precipitates from spinal cord mitochondria probed with the anti-human SOD1 antibody. The right panel shows a comparison of Bcl-2 precipitates from spinal cord and liver mitochondria isolated from a FALS-A4V patient. Western blot was probed with the anti-human SOD1 antibody.

(C) 10 μg of spinal cord and liver mitochondria isolated from SOD1$^{G93A}$ mice (left) and FALS-A4V patient (right) were resolved on SDS-PAGE, transferred to nitrocellulose, and blotted with the anti-human SOD1 antibody.

Asterisks indicate high molecular weight SDS-resistant SOD1 containing aggregates. Abbreviations: SC, spinal cord; LV, liver.

spinal cords, we found that the anti-Bcl-2 antibody coprecipitated only mutant but not SOD1$^{WT}$ (Figures 7A and 7B), even though Bcl-2 was successfully precipitated in all mouse samples (Figure 7A, bottom). Together with monomeric SOD1, the Bcl-2 antibody coprecipitated high molecular weight SDS-resistant aggregates containing mutSOD1 (Figures 7A and 7B). Moreover, these aggregated forms of mutSOD1 were pulled down with the anti-Bcl-2 antibody in spinal cord but not in liver mitochondria (Figures 7A and 7B). These results are not a consequence of different levels of SOD1 expression in these tissues, as SOD1 is equivalently expressed in spinal cord and liver mitochondria (Figure 7C). However, they suggest a correlation between the motor neuron phenotype of the disease and the formation of the SOD1/Bcl-2-containing aggregates. We note that high molecular weight SDS-resistant SOD1- and Bcl-2-positive aggregates similar to those in human A4V and mouse G93A spinal cord mitochondria were also detected in spinal cord mitochondria from SOD1$^{G37R}$ transgenic ALS mice (Supplemental Figure S1 at http://www.neuron.org/cgi/content/full/43/1/19/DC1).

## Discussion

In transgenic ALS mice, it is evident that multiple processes converge to reduce motor neuron viability in an age-dependent manner. As gauged temporally, these include early mitochondrial vacuolization (Wong et al., 1995), activation of microglial proliferation, and concomitant activation of caspase-1 (Pasinelli et al., 2000). Later stages entail aggregation of mutSOD1 protein (Bruijn et al., 1998), activation of caspase-3 (Pasinelli et al., 2000), and motor neuronal cell death. These events unfold in the setting of enhanced sensitivity to excitotoxic stimuli associated with failure of astroglial glutamate transport (Rothstein et al., 1990), perturbed oxidative metabolism as measured by levels of diverse oxidative species, and gradual failure of energy generation and mitochondrial function (Bowling et al., 1993). Despite intensive investigation, the mechanisms whereby mutSOD1 protein triggers and sustains these events has remained elusive. Equally problematic has been the explanation for how mutations in a ubiquitously expressed and abundant protein produce a cell death process that is so exquisitely motor neuron specific.

The present study provides new insight into these questions by delineating a direct binding interaction between wt or mutSOD1 and the anti-apoptotic protein Bcl-2. This interaction is readily demonstrated both in vitro and in vivo in mouse and human spinal cords. The binding is specific; neither Actin nor the pro-apoptotic protein Bax co-immunoprecipitate with SOD1. Our data show that ALS-associated mutSOD1 protein binds avidly to mitochondria with which it forms SDS-resistant aggregates that, in turn, are bound by and contain Bcl-2. We also report comparable association between SOD1/Bcl-2-positive aggregates and mitochondria in the spinal cord of a patient who succumbed to familial ALS caused by the very common alanine-4-valine mutation. In our view, it is striking that both in the ALS mice and FALS-A4V patient, these SOD1/Bcl-2-containing aggregates are readily detected in spinal cord mitochondria but are absent in liver mitochondria. These observations argue that one important mechanism for the neurotoxicity of mutSOD1 protein may derive from adverse consequences of this mutant protein on the function of Bcl-2 and mitochondria. Figure 8 summarizes these findings.

That mitochondrial pathology is an essential element in neuronal cell death in transgenic ALS mice seems

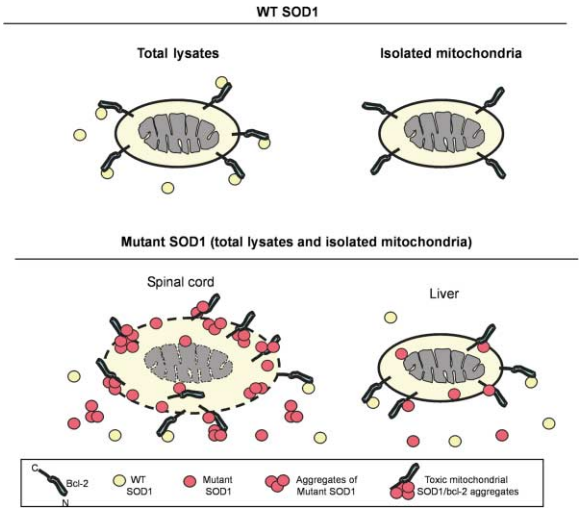


Figure 8. Schematic Model of the SOD1/Bcl-2 Interaction

Top: SOD1$^{WT}$ binds to the N-terminal domain of Bcl-2 that is located in the cytosol. Our data indicate that the binding is disrupted during mitochondria isolation. Bottom: The unstable mutant SOD1 protein forms insoluble aggregates that bind Bcl-2 and are strongly associated with the outer membrane of the mitochondria. mutSOD1 is present in purified mitochondria under the same preparative conditions used for SOD1$^{WT}$. The high molecular weight mutSOD1/Bcl-2 aggregates are present in spinal cord mitochondria but not liver mitochondria.

irrefutable. As assessed by both functional and morphological criteria, mitochondrial damage is a characteristic feature of motor neuron degeneration mediated by mutSOD1 protein. In ALS transgenic mice, mitochondrial degeneration and vacuolization are among the earliest abnormalities, detected well before signs of clinical motor weakness; the peak of this vacuolization coincides with onset of weakness in the G93A transgenic mice (Wong et al., 1995; Kong and Xu, 1998). Biochemical analyses document that mitochondrial respiratory chain activity and ATP generation are diminished in the presence of mutSOD1 (Mattiazzi et al., 2002). As estimated histochemically, electron transport function is reduced in the ALS mice, specifically in the ventral horns (Higgins et al., 2002). Furthermore, there is evidence that calcium homeostasis and membrane potential are significantly perturbed in mitochondria from the ALS mice (Appel et al., 2001). That mitochondria are particularly sensitive to the presence of mutSOD1 has been confirmed in quantitative estimates of cell death arising from targeting of SOD1 specifically to the nucleus, cytosol, and mitochondrion (Takeuchi et al., 2002).

The mechanism for the particular susceptibility of mitochondria to mutSOD1 has not been explained. An important clue is provided by several studies in the last five years showing that in yeast, mice, and rats, a fraction of the normally cytosolic SOD1 protein is detected within the mitochondrion, probably either at the surface of this organelle or within its intermembrane space (Sturtz et al., 2001; Higgins et al., 2002; Okado-Matsumoto and Fridovich, 2002; Mattiazzi et al., 2002). From an evolutionary perspective, this is not surprising given that the primary cellular site for the generation of superoxide anion, the substrate of SOD1, is in the outer mitochondria via the activity of the respiratory chain complexes. The route of entry and process by which cytosolic SOD1 is imported into mitochondria are not known. Nonetheless, these studies collectively raise the hypothesis that an important element in mitochondrial dysfunction in the ALS mice is the intimate spatial relationship between this organelle and mutSOD1 protein.

The present study reveals that at least one pathway whereby SOD1 interacts with the mitochondrion is by binding and docking to Bcl-2. In vitro, this is evident with both wt and mutSOD1. This observation is compatible with reports that wt and mutSOD1 can enter the mitochondrion (Mattiazzi et al., 2002; Okado-Matsumoto and Fridovich, 2002). Moreover, this finding potentially provides a link between a normal docking function and the evolution of mitochondrial pathology. It is clear from numerous studies that one pathogenic feature of mutated SOD1 is diminished protein stability and a proclivity to aggregate (Cleveland and Rothstein, 2001). We now report that aggregates of SOD1 are abundant and readily detected in spinal cord mitochondria. It is plausible that the localization of SOD1 to the mitochondrion via the Bcl-2 interaction, either on the outside or just within the outer membrane, positions the mutant protein to aggregate in a manner that is toxic to the mitochondrion. We note that other groups have also described high molecular weight species of mutSOD1 protein in mitochondria (Mattiazzi et al., 2002).

Moreover, these findings point to a link between the pattern of mitochondrial SOD1 aggregation and the motor neuron focus of ALS. For reasons that are not clear as yet, the process of accumulation of aggregates in mitochondria is evident in spinal cord but not liver mitochondria. To the extent that aggregates or proto-aggregates of mutSOD1 are toxic to mitochondria, this preferential aggregation of SOD1 in spinal cord but not liver mitochondria defines a potential Achilles' heel that may render spinal cord cells susceptible to this mutant protein. These studies are consonant with recent data demonstrating that mutant but not SOD1$^{WT}$ specifically localizes to spinal cord mitochondria of ALS mice and patients (D.W. Cleveland, International ALS/MND meeting, Milan, Italy, 2003).

We note that by contrast with our findings, Mattiazzi and colleagues reported that both wt and mutSOD1 bind to the intermembrane space of the mitochondria (Mattiazzi et al., 2002). We have found that SOD1$^{WT}$ binds to Bcl-2 but do not find evidence that the wt molecule is present in isolated mitochondria. We think that this discrepancy reflects differences in our assays. Because our detection system required immunoprecipitation, we should have detected even minute amounts of residual SOD1$^{WT}$ in the purified mitochondria. The failure to do so strongly suggests that SOD1$^{WT}$ is not present in the isolated mitochondrion. It is conceivable that less stringent systems for the purification of the mitochondrion and detection of the SOD1/Bcl-2 interaction may entail residual contamination by cytosolic SOD1.

How do the mitochondrial mutSOD1/Bcl-2-containing aggregates cause toxicity? Bcl-2 is a major regulator of mitochondrial integrity and mitochondrial-initiated caspase activation. Two important functions have been proposed for Bcl-2 in the mitochondria: the regulation of the mitochondrial membrane potential and the binding

and inhibition of pro-apoptotic proteins (Danial and Korsmeyer, 2004). It is known that protein-protein interactions play an important role in the function of Bcl-2. Members of the Bcl-2 family regulate apoptosis either through homodimerization, heterodimerization with proteins in the same family, or binding with other protein partners. One possible consequence of the binding of Bcl-2 to SOD1 may be that Bcl-2 itself will effectively be entrapped and rendered nonfunctional as the mutSOD1 protein aggregates. To the extent that Bcl-2 also actively binds other anti-apoptotic proteins, this process of segregation may further render the mitochondrion and its host cell less viable. This proposal is analogous to the suggestion that aggregated SOD1 might serve as a sink for heat shock proteins, thereby increasing the pro-apoptotic state of the mitochondrion (Okado-Matsumoto and Fridovich, 2002). Entrapment of Bcl-2 into mutSOD1 aggregates may also inhibit heterodimerization of Bcl-2 with pro-apoptotic molecules, a process that normally blocks apoptosis. We note that in isolated mitochondria from the spinal cord of an A4V ALS patient, coprecipitates of mutSOD1 and Bcl-2 do not contain the pro-apoptotic protein Bax (unpublished observations). Published data are consistent with the idea that entrapped Bcl-2 cannot form Bcl-2/Bax heterodimers that normally block Bax pro-apoptotic function. In the $SOD1^{G93A}$ mice, Bcl-2 expression decreases during the course of the disease; this parallels an increase in Bax expression and a decrease in Bcl-2/Bax heterodimers (Vukosavic et al., 1999).

This hypothesis is consonant with studies documenting that Bcl-2 is a prosurvival protein that is required by mature motor neurons (Michaelidis et al., 1996). In mice with genetically inactivated Bcl-2, developmental loss of motor neurons by apoptosis occurs normally. However, after early periods of fetal development, these mice show accelerated death of motor and sensory neurons. This indicates that other anti-apoptotic members of the Bcl-2 gene family do not fully compensate for the absence of Bcl-2. The fact that total loss of Bcl-2 causes death of both motor and sensory neurons, while mutSOD1 initiates selective motor neuron death, may reflect two points. First, the mutSOD1-dependent reduction in Bcl-2 is partial and slowly progressive. Second, motor neurons at baseline show reduced expression of Bcl-2 compared to sympathetic and sensory neurons (Yachnis et al., 1998) and thus may be more sensitive to partial loss of Bcl-2. Taking these considerations together, we find it plausible that mutSOD1-related reduction in levels of Bcl-2 can compromise motor neuron viability.

Another possible consequence of the binding of mutSOD1 to Bcl-2 is that this interaction may induce a conformational change that converts Bcl-2 into a pro-apoptotic molecule. This mechanism is suggested by the recent report that an interaction between the nuclear orphan receptor Nur77/TR3 and Bcl-2 induces conformational modifications of Bcl-2 that convert it into a killer protein (Lin et al., 2004).

Details of the biophysical nature of the SOD1-Bcl-2 interaction await further analysis. As noted, our experiments strongly indicate that mutSOD1 is associated with Bcl-2 within or at the surface of the mitochondrion. Bcl-2 is a membrane protein anchored to the outer membrane of the mitochondria in an $N_{cytosol}$-$C_{mitochondria}$ orientation, leaving the majority of the protein reaching into the cytosol. Our in vitro data with Bcl-2 deletion mutants show that $SOD1^{WT}$ binds the cytosolic portion of Bcl-2. In vivo, the ionic strength of the mitochondria isolation buffer is sufficient to disrupt this binding. On the contrary, the binding between mutSOD1 and Bcl-2 is stable in the same buffer. Moreover, our data suggest that mutSOD1 does not exclusively bind the N terminus. Because we find mutSOD1 in the purified, isolated mitochondria, we believe that the mutated protein binds the carboxy-terminal domain of Bcl-2. Whether such docking is required for subsequent translocation into the mitochondrion and the mechanism of translocation are not known. Okado-Matsumoto and Fridovich reported that in mouse neuroblastoma N2A cells, the entry of both wt and mutSOD1 into the mitochondria depends on demetallation. While partially or fully demetallated SOD1 is integrated into the mitochondrion, the holoenzyme is not. Noted in this context are reports that demetallation of mutSOD1 accentuates its neurotoxic properties in neurons in vitro (Estevez et al., 1999). Conceivably, our observation that in ALS patients and transgenic ALS mice only the mutant protein enters the mitochondrion may reflect the fact that only the mutant protein is sufficiently conformationally unstable to lose metals.

Like Bcl-2, $SOD1^{WT}$ is anti-apoptotic in neurons. SOD1 delays neuronal apoptosis in cultured sympathetic neurons (Greenlund et al., 1995). Downregulation of SOD1 expression in cultured spinal motor neurons provokes apoptotic cell death and it enhances the sensitivity of PC12 and immortalized rat nigral neuronal cells to various apoptotic stimuli (Rothstein et al., 1994; Troy and Shelanski, 1994). Similarly, primary motor neurons derived from SOD1 knockout mice undergo apoptosis and exhibit enhanced cell death after axonal injury. Because SOD1 represents one of the major anti-oxidant defenses in the cells and production of reactive oxygen species (ROS) and oxidative stress have been implicated in apoptosis, the anti-apoptotic properties of SOD1 have mainly been attributed to its anti-oxidant activity. A fundamental question that therefore follows from this study is whether the anti-apoptotic properties of SOD1 are a consequence of both its dismutase/anti-oxidant function and, in parallel but perhaps independently, its interaction with Bcl-2. That the dismutation function of SOD1 can be dissociated from its anti-apoptotic properties is clear from studies showing that different mutant alleles of SOD1 retain nearly normal dismutation activity but are pro-apoptotic in cells in culture (Pasinelli et al., 1998). This is consistent with the report that injection of $SOD1^{WT}$ or Bcl-2 expression vectors into immortalized rat nigral neuronal cells delayed apoptosis induced by NGF withdrawal but did not completely block cell death, even though SOD1 expression blocked ROS formation (Rabizadeh et al., 1995). The implication, therefore, is that the anti-apoptotic function of $SOD1^{WT}$ is likely to reflect some other activity. We raise the possibility that one such activity is the binding of SOD1 to the best-defined anti-apoptotic protein, Bcl-2. An intriguing reciprocal question is whether the anti-apoptotic properties of Bcl-2 are in some way contingent on its binding to SOD1. There are few data with which to judge this possibility at this time. However, the availability of mice and worms

devoid of SOD1 should allow the design of experiments to test this concept.

## Experimental Procedures

### Cell Culture and Reagents

N2A cell cultures stably transfected with wt and mutant (G37R, G41D, and G85R) SOD1 were grown in medium containing 50% DMEM, 50% OPTI-MEM, 7% fetal bovine serum, 1% antibiotic antimycotic, and 400 μg/ml of the neomycin analog G418. Cells were harvested for co-immunoprecipitation experiments at 80% confluency. The anti-mouse Bcl-2 polyclonal antibody used for immunoprecipitation was obtained from Research Diagnostics, Inc. (RDI). The anti-mouse polyclonal antibody used for Western blot analysis was from Pharmingen. Antibodies used for immunoprecipitation and Western blot analysis of human Bcl-2 were obtained from Biosource, Oncogene, and Santa Cruz. Rabbit anti-human SOD1 antibodies were from Biodesign and from Calbiochem. The anti-FLAG antibody was from Stratagene (La Jolla, CA). For FLIM analysis, fluorescein-conjugated anti-hamster antibody and Cy$^{TM3}$-conjugated anti-rabbit secondary antibodies were from Vector Laboratories (Burlingame, CA) and Jackson Immunoresearch Laboratories, respectively. Human Bcl-2 wt and mutant cDNAs were kindly provided by Dr. Stanley Korsmeyer (Dana Farber Institute, Boston, MA). The pcMV-FLAG-tag vector was from Stratagene. The TNT Quick Coupled Transcription/Translation System used for in vitro transcription-translation of Bcl-2 and SOD1 was from Promega.

### Co-Immunoprecipitations

N2A cells were lysed in radio immunoprecipitation assay (RIPA) buffer (50 mM Tris-HCl [pH 8.0], 150 mM NaCl, 1% NP-40, 12 mM deoxycolic acid) containing proteases inhibitors (Boeringher Mannheim). After centrifugation (3500 × g, 20 min, 4°C), supernatants were precleared for 8 hr at 4°C with Biomag Protein A magnetic beads (Qiagen, Valencia, CA). Rabbit anti-mouse Bcl-2 primary antibody (2.5 μg) or rabbit anti-human SOD1 primary antibody (5 μg) were then added to the lysates and incubated overnight at 4°C. The antibody-antigen complex was then precipitated with Protein A magnetic beads (4 hr, 4°C, with rotation). Immunoprecipitates were washed three times with 200 μl of RIPA buffer, 20 μl of reducing sample buffer were added to the final pellet, and samples were boiled. Beads were pulled down using a magnet, supernatant was loaded on a 15% SDS-PAGE for electrophoresis, and Western blot analysis was followed by enhanced chemiluminescence using the Amersham ECL system.

For immunoprecipitation of mouse or human spinal cord, samples were homogenized in RIPA buffer containing protease inhibitors and immunoprecipitation was carried out as described above. In the human samples, an anti-human Bcl-2 antibody was used.

### Crosslinking Analysis and Two-Dimension Electrophoresis

The hydrophobic crosslinker DSP (Pierce, Rockford, IL; 5 mg/ml in DMSO) was used. 1 mg of N2A cell lysates were incubated for 30 min at room temperature with 0, 0.5, or 2 mM DSP in a final volume of 500 μl, buffered with PBS (pH 7.4). The reaction was stopped with 1 M Tris-HCl, and 500 μl of 2× nonreducing sample buffer were added to each sample. Samples were boiled for 10 min prior to analysis in the first dimension SDS-PAGE. The position of high molecular mass complexes was analyzed in the first dimension by Western blot analysis using antibodies to either mouse Bcl-2 or human SOD1. First dimension lanes were excised from unstained, unfixed gels, reduced in β-mercapto-ethanol, and laid on top of the second dimension SDS-PAGE and proteins resolved under reducing conditions. Gels were silver stained using a GelCode SilverSNAP kit (Pierce). Immunoblots replicas were incubated with antibodies to either mouse Bcl-2 or human SOD1.

### Fluorescence Lifetime Imaging Microscopy

N2A cells were fixed in PBS containing 4% paraformaldehyde for 10 min, washed twice with PBS, and incubated with PBS containing 5% Glycine for 10 min. Cells were blocked and permeabilized in PBS containing 10% goat serum, 5% bovine serum albumine (BSA), and 0.5% Triton X (v/v). Cells were incubated first with the anti-Bcl-2 antibody (overnight, 4°C) and then with the anti-SOD1 or Cox4 antibody (room temperature, for 60 min). Prior to addition of the fluoro-labeled secondary antibodies, cells were washed three times in PBS. Baseline decay times for FLIM were gathered as previously described (Bacskai et al., 2003) by using the 488 fluorescein flouorophore attached to either the primary anti-Bcl-2 antibody or a fluorescent secondary antibody. Decay times were measured using a multiphoton microscope (Radiance 2000, Bio-Rad) with a Ti:Saphire laser (Tsunami, Spectra Physics) and a fast microchannel plate detector (MCP; Hamamatsu, Bridgewater, NJ) connected to high-speed time correlated single photon counting (TCSPC) acquisition hardware (SPC-830; Becker & Hickl, Berlin) and data analyzed using a SPCImage software (Becker & Hickl). To investigate colocalization between Bcl-2 and SOD1, spinal cord sections from human SOD1$^{WT}$ overexpressing mice were double labeled using secondary immunofluoresence with fluorescein and Cy3 for Bcl-2 and SOD1, respectively. Images were collected using a Nikon Eclipse E800M microscope (Nikon, Mellville, NY) and Spot RT Software (Sterling Heights, MI).

### In Vitro Transcription-Translation

Plasmids containing the T7 promoter were transcribed and translated in reticulocytes lysates (TNT coupled system; Promega) following the manufacturer's instructions. When [$^{35}$S]methionine was used, proteins were translated for 1 hr in the presence of [$^{35}$S]methionine. Reticulocyte lysates containing translated proteins were immunoprecipiated using anti-human Bcl-2 antibodies or anti-human SOD1 antibody, and immunoprecipitation was carried out as described above. Immunoprecipitated proteins were resolved on SDS-PAGE, transferred to nitrocellulose, and analyzed by Western blot analysis. [$^{35}$S]methionine radiolabeled proteins were visualized by autoradiography.

### Expression of Bcl-2 and SOD1 in *Xenopus laevis* Oocytes

The ΔBH4 Bcl-2 deletion mutant and the ΔBH4/Δloop Bcl-2 double deletion mutant were subcloned into a pCMV-Tg4 vector (Stratagene) containing a N-terminal FLAG and transcribed in vitro using the mMessage mMachine Kit (Ambion). Linearized human SOD1 (wt and mutants) containing plasmids were similarly transcribed. Stage V *Xenopus laevis* oocytes were enzymatically defolliculated, injected with *bcl-2* cRNAs (20 ng/50 nl/oocyte) in combination with wt or mutSOD1 cRNAs (20 ng/50 nl/oocyte), and maintained at 18°C in L-15 solution (Specialty Media) supplemented with gentamycin sulfate (100 μg/ml). 3 days postinjection, oocytes were solubilized in RIPA buffer containing protease inhibitors; human Bcl-2 and human SOD1 were co-immunoprecipitated using a monoclonal anti-FLAG antibody (Stratagene). Proteins were resolved on SDS-PAGE, transferred to nitrocellulose, and analyzed by Western immunoblotting.

### Mitochondria Isolation

Mouse and human liver and spinal cord were homogenized in Buffer A containing 70 mM sucrose, 190 mM mannitol, 20 mM HEPES, and 0.2 mM EDTA (pH 7.5) in a glass-Teflon pestle. The homogenate was centrifuged at 650 × g for 10 min. The resulted supernatant was centrifuged at 7700 × g for 10 min. The resulted supernatant was centrifuged at 100,000 × g to collect the cytosolic fraction while the pellet was resuspended in Buffer A and centrifuged again at 7700 × g for 10 min. The resulting mitochondrial pellet was resuspended in 200 μl of immunoprecipitation buffer containing protease inhibitors.

### Acknowledgments

We thank Dr. Stanley Korsmeyer for the generous gift of the Bcl-2 deletion mutants and Dr. Jeffrey Rothstein for providing spinal cords of SOD1$^{G37R}$ mice. Rodrigo Ferreira is acknowledged for technical assistance. This work was supported by the Spinal Cord Research Foundation, Project ALS, and the Muscular Dystrophy Association (P.P.); the Pierre L. Bourgknecht ALS Foundation and Project ALS (R.H.B.); NIH grants RO3-AG022252 (P.P.), RO1-NS44292 (D.T.), PO1 AG12992-9 (R.H.B.), EB00768 (B.J.B.), and R37 AG12406 (B.T.H.); and Pioneer Award from the Alzheimer Association (B.T.H.).

Received: February 10, 2004
Revised: April 13, 2004
Accepted: June 17, 2004
Published: July 7, 2004

## References

Andersen, P.M., Sims, K.B., Xin, W.W., Kiely, R., O'Neill, G., Ravits, J., Pioro, E., Harati, Y., Brower, R.D., Levine, J.S., et al. (2003). Sixteen novel mutations in the Cu/Zn superoxide dismutase gene in amyotrophic lateral sclerosis: a decade of discoveries, defects and disputes. Amyotroph. Lateral Scler. Other Motor Neuron Disord. *4*, 62–73.

Appel, S.H., Beers, D., Siklos, L., Engelhardt, J.I., and Mosier, D.R. (2001). Calcium: the Darth Vader of ALS. Amyotroph. Lateral Scler. Other Motor Neuron Disord. *2* (*Suppl 1*), S47–S54.

Bacskai, B.J., Skoch, J., Hickey, G.A., Allen, R., and Hyman, B.T. (2003). Fluorescence resonance energy transfer determinations using multiphoton fluorescence lifetime imaging microscopy to characterize amyloid-beta plaques. J. Biomed. Opt. *8*, 368–375.

Bowling, A.C., Schulz, J.B., Brown, R.H.J., and Beal, M.F. (1993). Superoxide dismutase activity, oxidative damage and mitochondrial energy metabolism in familial and sporadic amyotrophic lateral sclerosis. J. Neurochem. *61*, 2322–2325.

Bruijn, L.I., Houseweart, M.K., Kato, S., Anderson, K.L., Anderson, S.D., Ohama, E., Reaume, A.G., Scott, R.W., and Cleveland, D.W. (1998). Aggregation and motor neuron toxicity of an ALS-linked SOD1 mutant independent from wild-type SOD1. Science *281*, 1851–1854.

Cleveland, D.W., and Rothstein, J.D. (2001). From Charcot to Lou Gehrig: deciphering selective motor neuron death in ALS. Nat. Rev. Neurosci. *2*, 806–819.

Dal Canto, M., and Gurney, M. (1995). Neuropathological changes in two lines of mice carrying a transgene for mutant human Cu, Zn SOD, and in mice overexpressing wild type human SOD: a model of familial amyotrophic lateral sclerosis. Brain Res. *676*, 25–40.

Danial, N.N., and Korsmeyer, S.J. (2004). Cell death. Critical control points. Cell *116*, 205–219.

Durham, H., Roy, J., Dong, L., and Figlewicz, D. (1997). Aggregation of mutant Cu/Zn superoxide dismutase proteins in a culture model of ALS. J. Neuropathol. Exp. Neurol. *56*, 523–530.

Ekegren, T., Grundstrom, E., Lindholm, D., and Aquilonius, S.M. (1999). Upregulation of Bax protein and increased DNA degradation in ALS spinal cord motor neurons. Acta Neurol. Scand. *100*, 317–321.

Estevez, A.G., Crow, J.P., Sampson, J.B., Reiter, C., Zhuang, Y., Richardson, G.J., Tarpey, M.M., Barbeito, L., and Beckman, J.S. (1999). Induction of nitric oxide-dependent apoptosis in motor neurons by zinc-deficient superoxide dismutase. Science *286*, 2498–2500.

Friedlander, R., Brown, R.H., Jr., Gagliardini, V., Wang, J., and Wang, J. (1997). Inhibition of ICE slows ALS in mice. Nature *388*, 31.

Ghadge, G., Lee, J., Bindokas, V., Jordan, J., Ma, L., Miller, R., and Roos, R. (1997). Mutant superoxide dismutase-1-linked familial amyotrophic lateral sclerosis: molecular mechanisms of neuronal death and protection. J. Neurosci. *17*, 8756–8766.

Greenlund, L., Deckwerth, T., and Johnson, E. (1995). Superoxide dismutase delays neuronal apoptosis: a role for reactive oxygen species in programmed neuronal death. Neuron *14*, 303–315.

Guegan, C., and Przedborski, S. (2003). Programmed cell death in amyotrophic lateral sclerosis. J. Clin. Invest. *111*, 153–161.

Guegan, C., Vila, M., Rosoklija, G., Hays, A.P., and Przedborski, S. (2001). Recruitment of the mitochondrial-dependent apoptotic pathway in amyotrophic lateral sclerosis. J. Neurosci. *21*, 6569–6576.

Higgins, C.M., Jung, C., Ding, H., and Xu, Z. (2002). Mutant Cu, Zn superoxide dismutase that causes motoneuron degeneration is present in mitochondria in the CNS. J. Neurosci. *22*, RC215.

Ilzecka, J., Stelmasiak, Z., and Dobosz, B. (2001). Interleukin-1beta converting enzyme/Caspase-1 (ICE/Caspase-1) and soluble APO-1/Fas/CD 95 receptor in amyotrophic lateral sclerosis patients. Acta Neurol. Scand. *103*, 255–258.

Kong, J., and Xu, Z. (1998). Massive mitochondrial degeneration in motor neurons triggers the onset of amyotrophic lateral sclerosis in mice expressing a mutant SOD1. J. Neurosci. *18*, 3241–3250.

Kostic, V., Jackson-Lewis, V., de Bilbao, F., Dubois-Dauphin, M., and Przedborski, S. (1997). Bcl-2: prolonging life in a transgenic mouse model of familial amyotrophic lateral sclerosis. Science *277*, 559–562.

Li, M., Ona, V.O., Guegan, C., Chen, M., Jackson-Lewis, V., Andrews, L.J., Olszewski, A.J., Stieg, P.E., Lee, J.P., Przedborski, S., and Friedlander, R.M. (2000). Functional role of caspase-1 and caspase-3 in an ALS transgenic mouse model. Science *288*, 335–339.

Lin, B., Kolluri, S.K., Lin, F., Liu, W., Han, Y.H., Cao, X., Dawson, M.I., Reed, J.C., and Zhang, X.K. (2004). Conversion of Bcl-2 from protector to killer by interaction with nuclear orphan receptor Nur77/TR3. Cell *116*, 527–540.

Martin, L.J. (1999). Neuronal death in amyotrophic lateral sclerosis is apoptosis: possible contribution of a programmed cell death mechanism. J. Neuropathol. Exp. Neurol. *58*, 459–471.

Mattiazzi, M., D'Aurelio, M., Gajewski, C.D., Martushova, K., Kiaei, M., Beal, M.F., and Manfredi, G. (2002). Mutated human SOD1 causes dysfunction of oxidative phosphorylation in mitochondria of transgenic mice. J. Biol. Chem. *277*, 29626–29633.

Michaelidis, T.M., Sendtner, M., Cooper, J.D., Airaksinen, M.S., Holtmann, B., Meyer, M., and Thoenen, H. (1996). Inactivation of bcl-2 results in progressive degeneration of motoneurons, sympathetic and sensory neurons during early postnatal development. Neuron *17*, 75–89.

Okado-Matsumoto, A., and Fridovich, I. (2002). Amyotrophic lateral sclerosis: a proposed mechanism. Proc. Natl. Acad. Sci. USA *99*, 9010–9014.

Parkes, T.L., Elia, A.J., Dickinson, D., Hilliker, A.J., Phillips, J.P., and Boulianne, G.L. (1998). Extension of *Drosophila* lifespan by overexpression of human SOD1 in motorneurons. Nat. Genet. *19*, 171–174.

Pasinelli, P., Borchelt, D.R., Houseweart, M.K., Cleveland, D.W., and Brown, R.H., Jr. (1998). Caspase-1 is activated in neural cells and tissue with amyotrophic lateral sclerosis-associated mutations in copper-zinc superoxide dismutase. Proc. Natl. Acad. Sci. USA *95*, 15763–15768.

Pasinelli, P., Houseweart, M.K., Brown, R.H., Jr., and Cleveland, D.W. (2000). Caspase-1 and -3 are sequentially activated in motor neuron death in Cu,Zn superoxide dismutase-mediated familial amyotrophic lateral sclerosis. Proc. Natl. Acad. Sci. USA *97*, 13901–13906.

Rabizadeh, S., Gralla, E., Borchelt, D., Gwinn, R., Valentine, J., Sisodia, S., Wong, P., Lee, M., Hahn, H., and Bredesen, D. (1995). Mutations associated with amyotrophic lateral sclerosis convert superoxide dismutase from an antiapoptotic gene to a proapoptotic gene: studies in yeast and neural cells. Proc. Natl. Acad. Sci. USA *92*, 3024–3028.

Rosen, D.R., Siddique, T., Patterson, D., Figlewicz, D.A., Sapp, P., Hentati, A., Donaldson, D., Goto, J., O'Regan, J.P., Deng, H.X., et al. (1993). Mutations in Cu/Zn superoxide dismutase gene are associated with familial amyotrophic lateral sclerosis. Nature *362*, 59–62.

Rothstein, J.D., Tsai, G.T., Kuncl, R.W., Clawson, L., Cornblath, D.R., Drachman, D.B., Pestronk, A., Stauch, B.L., and Coyle, J.T. (1990). Abnormal excitatory amino acid metabolism in amyotrophic lateral sclerosis. Ann. Neurol. *28*, 18–25.

Rothstein, J.D., Bristol, L.A., Hosler, B.A., Brown, R.H.J., and Kuncl, R.W. (1994). Chronic inhibition of superoxide dismutase produces apoptotic death of spinal neurons. Proc. Natl. Acad. Sci. USA *91*, 4155–4159.

Schimmer, A.D., Hedley, D.W., Penn, L.Z., and Minden, M.D. (2001). Receptor- and mitochondrial-mediated apoptosis in acute leukemia: a translational view. Blood *98*, 3541–3553.

Sedlak, T.W., Oltvai, Z.N., Yang, E., Wang, K., Boise, L.H., Thompson, C.B., and Korsmeyer, S.J. (1995). Multiple Bcl-2 family members

demonstrate selective dimerizations with Bax. Proc. Natl. Acad. Sci. USA *92*, 7834–7838.

Sturtz, L.A., Diekert, K., Jensen, L.T., Lill, R., and Culotta, V.C. (2001). A fraction of yeast Cu,Zn-superoxide dismutase and its metallochaperone, CCS, localize to the intermembrane space of mitochondria. A physiological role for SOD1 in guarding against mitochondrial oxidative damage. J. Biol. Chem. *276*, 38084–38089.

Takeuchi, H., Kobayashi, Y., Ishigaki, S., Doyu, M., and Sobue, G. (2002). Mitochondrial localization of mutant superoxide dismutase 1 triggers caspase-dependent cell death in a cellular model of familial amyotrophic lateral sclerosis. J. Biol. Chem. *277*, 50966–50972.

Troy, C.M., and Shelanski, M. (1994). Down-regulation of copper/zinc superoxide dismutase causes apoptotic death in PC12 neuronal cells. Proc. Natl. Acad. Sci. USA *91*, 6384–6387.

Vukosavic, S., Dubois-Dauphin, M., Romero, N., and Przedborski, S. (1999). Bax and Bcl-2 intercation in a transgenic mouse model of familial amyotrophic lateral sclerosis. J. Neurochem. *73*, 2460–2468.

Vukosavic, S., Stefanis, L., Jackson-Lewis, V., Guegan, C., Romero, N., Chen, C., Dubois-Dauphin, M., and Przedborski, S. (2000). Delaying caspase activation by Bcl-2: a clue to disease retardation in a transgenic mouse model of amyotrophic lateral sclerosis. J. Neurosci. *20*, 9119–9125.

Wong, P., Pardo, C., Borchelt, D., Lee, M., Copeland, N., Jenkins, N., Sisodia, S., Cleveland, D., and Price, D. (1995). An adverse property of a familial ALS-linked SOD1 mutation causes motor neuron disease characterized by vacuolar degeneration of mitochondria. Neuron *14*, 1105–1116.

Yachnis, A.T., Giovanini, M.A., Eskin, T.A., Reier, P.J., and Anderson, D.K. (1998). Developmental patterns of BCL-2 and BCL-X polypeptide expression in the human spinal cord. Exp. Neurol. *150*, 82–97.

Yin, X.M., Oltvai, Z.N., and Korsmeyer, S.J. (1994). BH1 and BH2 domains of Bcl-2 are required for inhibition of apoptosis and heterodimerization with Bax. Nature *369*, 321–323.